Journal of Physics: Conference Series **641** (2015) 012007 doi:10.1088/1742-6596/641/1/012007

ALR – Laser altimeter for the ASTER deep space mission. Simulated operation above a surface with crater

A G V de Brum[1], F C da Cruz[2] and A Hetem Jr[1]

[1] Universidade Federal do ABC – UFABC, Santo André, SP, Brazil
[2] Universidade de Campinas – UNICAMP/IFGW, Campinas, SP, Brazil

E-mail: antonio.brum@ufabc.edu.br

Abstract. To assist in the investigation of the triple asteroid system 2001-SN263, the deep space mission ASTER will carry onboard a laser altimeter. The instrument was named ALR and its development is now in progress. In order to help in the instrument design, with a view to the creation of software to control the instrument, a package of computer programs was produced to simulate the operation of a pulsed laser altimeter with operating principle based on the measurement of the time of flight of the travelling pulse. This software Simulator was called *ALR_Sim*, and the results obtained with its use represent what should be expected as return signal when laser pulses are fired toward a target, reflect on it and return to be detected by the instrument. The program was successfully tested with regard to some of the most common situations expected. It constitutes now the main workbench dedicated to the creation and testing of control software to embark in the ALR. In addition, the Simulator constitutes also an important tool to assist the creation of software to be used on Earth, in the processing and analysis of the data received from the instrument. This work presents the results obtained in the special case which involves the modeling of a surface with crater, along with the simulation of the instrument operation above this type of terrain. This study points out that the comparison of the wave form obtained as return signal after reflection of the laser pulse on the surface of the crater with the expected return signal in the case of a flat and homogeneous surface is a useful method that can be applied for terrain details extraction.

1. Introduction

In the last years, many space missions dedicated to the investigation of small bodies of the solar system occurred, while others are still in progress or being planned. Among these, missions NEAR-Shoemaker (1996-2001), Hayabusa (2003-2010), Rosetta (in progress; scheduled to end in December 2015), Hayabusa 2 [1] (scheduled to launch in 2015).

For the most part, these and other missions that have not been mentioned carry on board at least one laser altimeter (laser rangefinder) as an instrument of scientific research (shape, topography, mass, etc.) and aid to navigation, in the phase of greater proximity to the target. As an example, the LIDAR, used in the Hayabusa mission [2, 3].

In general terms, these devices are used for determining the distance to the target, within their reach, which is done from the firing of laser pulses towards the target and the detection of signals that return after reflection on the target surface. As an instrument of scientific research, the shape of the pulse that returns after reflection on the surface contains information about the roughness (topography) of the lighted area. This information collected over wide areas of the target surface is used in the construction of a 3D model of the terrain.

Inserted in this sector of contemporary space exploration, the mission ASTER was planned in cooperation with Russia to be the first Brazilian deep space mission. This mission intends to investigate the triple asteroid 2001-SN263 and has its launch date previously planned for 2017 [4, 5].

Among the instruments that will take part in this mission, the laser altimeter, named ALR (ASTER Laser Rangefinder), is being designed to meet the mission objectives concerning the investigation of the shapes, surfaces topographies and masses of the asteroids, together with the calculation of their masses, in addition to supporting the proximity navigation. Reference [6] Brum et al (2011) contains more detailed information about the instrument design.

The ALR is planned to be a solid state pulsed laser of Nd: YAG, diode pumped and Q switched. The frequency of the light emitted is 1064 nm. The modeling and simulation of the operation of a laser altimeter with such features was the subject of a previous article [7]. These studies, still in progress, aim at the creation of the various subroutines that will compose the control software of the apparatus, to be embedded in the Signal Processing and Control (electronic) Unit of the instrument (SPCU). The simulation includes the instrument, its operation and the environment in which it will supposedly operate. The fundamentals involved in the operation of a laser altimeter and the investigation of surfaces with its use are deeply discussed in [8].

With use of the MATLAB environment [9], a software Simulator was created to serve as a laboratory useful in the understanding, implementation and testing of all the concepts involved in the detection of distances using instruments similar to the ALR. The *ALR_Sim* Simulator constitutes the main result of this effort and brings together all the programs previously created. For more details on the program, see [10].

This article describes the modeling performed and the simulations conducted with use of the *ALR_Sim*, in order to obtain and evaluate what should be the expected results of the instrument operation on a surface with crater, and for an emitted pulse with exponential characteristic, which more closely approximates the real pulse emitted by a Q-switched solid-state laser.

2. Modeling and simulation

The complete simulation steps were described in details in the cited papers. The Simulator package covers all major expected conditions involving the operation of the instrument, which are:

- the physical features of the instrument (parameters, specifications and transmitter-detector characteristics);
- the features of the environment where the instrument will operate;
- the physical features of the target surface.

2.1. Emitting pulse modeling

The emitted pulse model that best represents the Q-switched laser emission is given by the exponential distribution. This curve has emitted power rise led by a quadratic term, followed by exponential emission decay [11].

$$P_3 = Bt^2 \exp\left(-\frac{t-\tau}{\omega}\right), \quad (1)$$

In Equation (1), B is an adjusting factor for the peak value of the emitted power, τ and ω are adjusted curve parameters to obtain P_{max} = 1 kW, ω_p = 10 ns (pulse width at half maximum power).

The pulse modeling for the general case, i.e., when one chooses P_{max}, ω_p, t_{max} (time to reach maximum power) and t_f (the larger time span to complete the decay), keeping the exponential feature, demands the determination of proper values for B, τ and ω for any case, which represents a complex matter, once these variables are interdependent. To achieve this goal, in addition to $P_3(t)$, described previously, a second curve, $P_4(t)$, was created using a smoothed cubic spline applied to the points in Table 1, created to represent (model) the characteristics of the expected emitted pulse. These points were chosen to model perfectly the emitted pulse curve, according to the available knowledge of it

today. Any modifications or advances in this knowledge can be inserted here. The function "CSAPS" (smoothed cubic spline) of MATLAB was used for this purpose

Table 1. Points used to model the shape of the exponential emitted pulse.

t (s)	t_i	t_1	t_{max1}	t_{max2}	t_2	t_3	t_f
P (W)	0	$P_{max}/2$	P_{max}	P_{max}	$P_{max}/2$	0	0

In Table 1,

t_i - is the starting moment of emission of the laser pulse (defined by the user);

t_1 - is the moment (calculated) when the pulse reaches half of its peak power, $P_{max}/2$, in the rising part of the curve, considering exponential emission; t_1 is given by

$$t_1 = t_i - \omega_P \left[1 + exp\left(\frac{\omega_P}{2\omega}\right)\right]\left[1 - exp\left(\frac{\omega_P}{\omega}\right)\right]^{-1};$$

t_2 - is the moment when the pulse reaches half of its peak power, $P_{max}/2$, in the descent part of the exponential curve;

t_{max1} and t_{max2} – subdivisions of t_{max}, instant of time corresponding to the maximum power value; created to assure P_{max} as the maximum value of the adjusted curve, with $t_{max1} = t_{max} - 0.1dt$ and $t_{max2} = t_{max} + 0.1dt$;

t_3 and t_f – used to model de curve decay (more abrupt or less), $t_3 = t_2 + \omega_p$; and $t_f = t_3 + \omega_p$.

2.2. Surface with crater modeling

The modeling of the surface with crater followed the profile of the lunar impact crater Eudoxus [12]. A sample of 45 points of half of the crater profile was taken resulting in the set of points (X_{crat}, Z_{crat}). These, in turn, were used to adjust a curve of type "Gauss 5" smoothed (internal function of MATLAB). The smoothed curve adjusted to the points of the crater, z = f (x), $0 \leq x \leq 40$ km, was used to determine the surface of revolution around the +z-axis. The crater surface points were obtained from a grid of equally-spaced points in the xy-plane with x and y taken between -40 and +40 metric units (km, m, etc.). For each of the internal points within the grid, the value of z=f(x, y) was calculated.

The model of the "N reflective point sources of the incident light", created for this simulation [7, 9], requires the identification of a set of points on the surface to be taken as sources of the light that returns to the detector. The determination of these points was made by taking the intersection points between the straight lines connecting the instrument transmitter, located, in the adopted frame, at the point A = (0, 0, R), to each point $P_i = (x_i, y_i, 0)$, of the flat footprint (defined and calculated in [7]), when these lines are prolonged until they reach the surface z = f (x, y), representing the crater surface (below the flat surface). Each intersection determines a point $P_i' = (x_i', y_i', z_i')$ of the crater surface, $z_{crat} = f(x,y)$.

The solution of the system created from the equations of the crater and of the line *r*, from A to each point P_i of the flat footprint, offers the set of intersection points P_i', related to each point P_i. To calculate each of these points, the numeric solver of systems of equations available in MATLAB was used. The crater determined through these points is shown in Figure 1. In this case, the value of N (1396 points) is a consequence of the chosen (input) value for L, the side dimension of one element of area on the flat footprint.

The equations of the line ***r*** and of the crater are given, respectively, by (2) and (3),

$$\frac{x}{x_i} = \frac{y}{y_i} = -\frac{(z - R)}{R} \tag{2}$$

$$Z_{crat} = E_1 + E_2, \tag{3}$$

where E_1 and E_2 given by

$$E_1 = a_1 exp\left[-\left(\frac{g-b_1}{c_1}\right)^2\right] + a_2 exp\left[-\left(\frac{g-b_2}{c_2}\right)^2\right] + a_3 exp\left[-\left(\frac{g-b_3}{c_3}\right)^2\right],$$

$$E_2 = a_4 exp\left[-\left(\frac{g-b_4}{c_4}\right)^2\right] + a_5 exp\left[-\left(\frac{g-b_5}{c_5}\right)^2\right], \text{ with } g = (x^2 + y^2)^{\frac{1}{2}}.$$

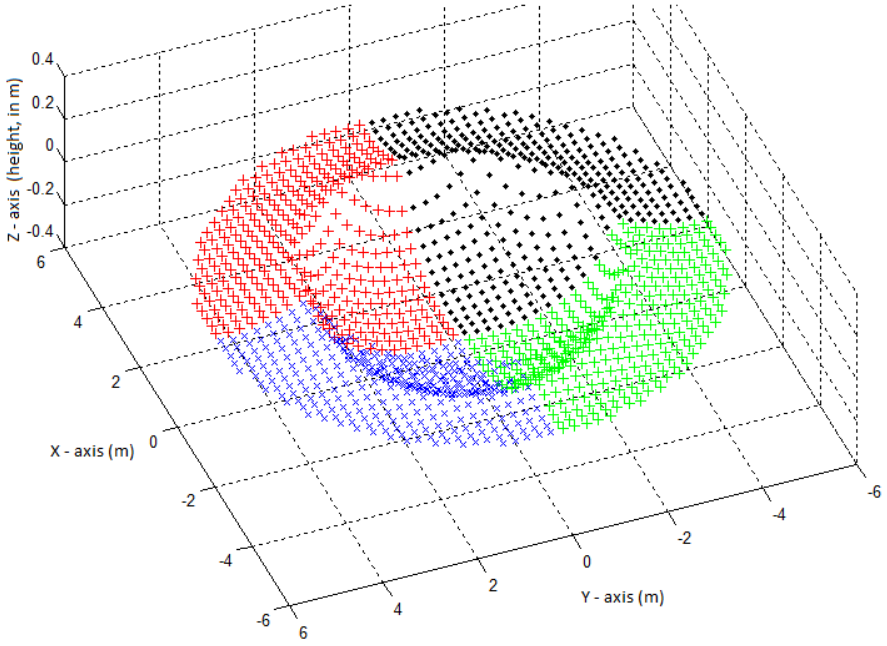

Figure 1. N=1396 point sources that reflect the light incident on the surface of the crater.

Once identified the points P_i', that are considered as emitting point sources of the light incident on the crater surface, one has also to calculate the cosine of the angle between the incident light and the normal to the surface at each point P_i'. This value is necessary for the purpose of calculating the intensity of the diffuse light that returns to the detector. Traditional methods in analytic geometry are used for this purpose. Thus,

$$\cos(\varphi) = \hat{n}_{vet} \cdot \hat{r}, \tag{6}$$

where $\hat{n}_{vet} = \vec{n}/|\vec{n}|$, $\vec{n} = \left(-\frac{\partial z}{\partial x}, -\frac{\partial z}{\partial y}, 1\right)$, z = z_{crat} and $\hat{r} = \vec{r}/|\vec{r}|$.

Identified the points P_i', i=1,...,N, and the angles between the normal to the surface at each point P_i' and the direction that returns to the detector, the contribution of each source of light from the surface of the crater can be calculated by the same procedure described before for other types of surfaces.

3. Results

An improved version of the *ALR_Sim* was created to include the functions related to the surface with crater. In the simulations performed, the following input data was used:

- Emitted pulse: exponential adjusted with 1,000 Watts of peak intensity and 10 ns in width (at half power);

- Emitter/detector altitude: 15,000 m;
- Approximate dimensions of target surface in the crater: 6 m diameter by 0.3 m depth;
- L=25 cm; side dimension of each element *dA* of the flat footprint area.

For the purpose of performing a comparative analysis, the results obtained with the same parameters in the case of a flat surface are presented in Figure 2.

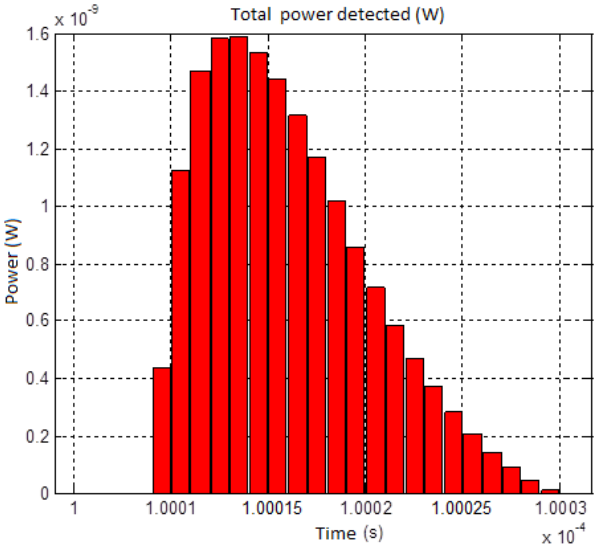

Figure 2(a). Response curve obtained from the return of the emitted light that reaches the flat footprint, distant 15 km from the transmitter, and returns to the receiver.

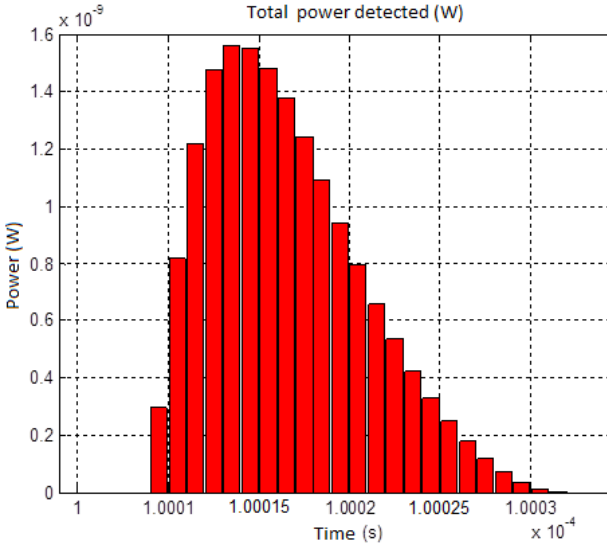

Figure 2(b). Response curve obtained in the case when the surface of the crater is illuminated centrally, in the same conditions of Figure 2(a).

It is observed here that the expected return signal, after reflection of the emitted pulse on a flat and homogeneous surface (constant reflectivity), should mirror the emitted pulse. Thus, the number of subdivisions in the sampling of the emitted pulse equals the number of subdivisions of the return signal (in Figure 2 (a), this means 21 subdivisions = 21 intervals 1 ns wide), the shape of the return wave follows the shape of the emitted wave, the intensity depends only on the distance and on the medium (reflectivity and absorption), the shortest distance between source and target is given by the time interval between the pulse emission starting moment, and the moment of arrival of the first return signal ($d_{min}=c*(t_{1r} - t_{1e})/2$), and the longest distance between source and target is given by the interval of time between the last sampled moment of pulse emission and the last moment of arrival of return signal ($d_{max}=c*(t_{fr} - t_{of})/2$). The difference between these two values gives the greatest difference of level of the lighted terrain. Of course, this account applied to the flat surface results null.

With regard to the surface with crater, the same emitted pulse is used to generate the same flat footprint. The rays of light coming from the emitter get through this plan and reach the surface of the crater, where they are identified as points of this surface and are considered as point sources of (part of) the incident light, as shown in Figure 1. Figure 2(b) shows the waveform obtained as return signal in this case. Comparing the two waveforms (Figure 2), their similarity is clear. Differences encountered are due to the crater features that can be, this way, extracted through a comparative analysis. Important items here to be analyzed are the differences in the power intensities which cause a "flattening" in the shape of the returning wave, and also the spread of this wave.

4. Conclusions and comments

The *ALR_Sim* Simulator was improved to include surfaces with crater and used to simulate the response of the operation of the instrument over one such surface. The models involved are presented

and the results show that this type of surface causes flattening and spreading in the waveform received, when the return signal is compared with the expected for a flat and homogeneous surface.

The comparative analysis used here is indicated as a useful method to the extraction of surface features and can be used also to understand and extract the details of any type of surface.

References

[1] Yano H 2012 Planetary protection of Hayabusa-2 mission, a sample return from 1999 JU3, C-type NEO. Presentation for the NASA Planetary Protection Subcommittee 2012. May 1-2, 2012 NASA Headquarters, Washington, D.C., USA

[2] Barnouin-Jha O S *et al* 2008 Small-scale topography of 25143 Itokawa from the Hayabusa laser altimeter. *Icarus* **198**, pp. 102-124. doi:10.1016/j.icarus.2008.05.026

[3] Tsuno K, Okumura E, Katsuyama Y, Mizuno T, Hassimoto T Nakayama M, Yuasa H 2006 Lidar on board asteroid explorer Hayabusa. *Proc. 6th Internat. Conf. on Space Optics (ESTEC, Noordwijk, The Netherlands, 27-30 June 2006*) *(ESA SP-621, June 2006)*

[4] Sukhanov A A, Velho H F C, Macau E E N, and Winter O C 2010 The Aster Project: Flight to a Near-Earth Asteroid. *Cosmic Research*. **48**, pp. 433-450

[5] Macau E E N, Winter O C, Velho, H F C, Sukhanov A A, Brum A G V de, Ferreira J L, Hetem Jr A, Sandonato G M and Sfair R 2011 The Aster Mission: Exploring for the First Time a Triple System Asteroid. *In: Proc. of the 62nd Int Astronautical Congress (Cape Town, South Africa, 2011)*

[6] Brum A G V de, Hetem Jr A, Rego I da S, Francisco C P F, Fenilli A, Madeira F, Cruz F C da, and Assafin M 2011 Preliminary Development Plan of the ALR, the Laser Rangefinder for the ASTER Deep Space Mission to the 2001-SN263 Asteroid. *Journal of Aerospace Technology and Management, JATM* **3**, p. 331-338. doi: 10.5028/jatm.2011.03033611.

[7] Brum A G V de, Rodrigues A P 2013 Topographic profile of a target with use of laser pulses. A survey directed to the Brazilian deep space mission ASTER. *Journal of Physics: Conf. Ser.* **465** 01 2003. doi:10.1088/1742-6596/465/1/012003.

[8] Shan J and Toth C K 2009 *Topographic Laser Ranging and Scanning: Principles and Processing* (Boca Raton: CRC Press)

[9] MATLAB Release 2009a, The MathWorks, Inc., Natick, Massachusetts, United States.

[10] Brum A G V de, Cruz, F C da, Hetem Jr A and Rodrigues A P 2014 ALR - A laser altimeter for the first Brazilian deep space mission. Modeling and simulation of the instrument and its operation. *Journal: Computational & Applied Mathematics* (Basel: Springer). doi: 10.1007/s40314-014-0145-8.

[11] Steinvall O 2000 Effects of target shape and reflection on laser radar cross sections. *Applied Optics*, **39**(24):4381–4391.

[12] Tolentino V 2014. Vaz Tolentino Lunar observatory. Retrieved from http://www.vaztolentino.com.br/imagens/6667-As-crateras-ARISTOTELES-e-EUDOXUS